


Research Article

Silver/Copper Nanoparticle-Modified Polymer Chitosan/PVA Blend Fibers

Dikeledi S. More,¹ Makwena J. Moloto ,^{1,2} Nosipho Moloto,³ and Kgabo P. Matabola⁴

¹Department of Chemistry, Faculty of Applied and Computer Sciences, Vaal University of Technology, Private Bag X021, Vanderbijlpark 1900, South Africa

²Institute of Nanotechnology and Water Sustainability, College of Science, Engineering and Technology, University of South Africa, Florida Park, Roodepoort 1709, South Africa

³School of Chemistry, Faculty of Science, Wits University, Private Bag 3, Johannesburg 2050, South Africa

⁴Nanotechnology Innovation Centre, Advanced Materials Division, Mintek, Private Bag X3015, Randburg 2125, South Africa

Correspondence should be addressed to Makwena J. Moloto; molotmj@unisa.ac.za

Received 19 April 2021; Accepted 15 June 2021; Published 1 July 2021

Academic Editor: Marta Fernández-García

Copyright © 2021 Dikeledi S. More et al. This is an open access article distributed under the Creative Commons Attribution License, which permits unrestricted use, distribution, and reproduction in any medium, provided the original work is properly cited.

In this study, chitosan (CS)/poly(vinyl alcohol) (PVA) (CS/PVA) blend nanofibers with varying weight ratios and silver (Ag)/copper (Cu)/CS/PVA composite fibers have been prepared successfully by the electrospinning process. The tip-to-collector distance was kept at 15 cm, and the applied voltage was varied from 15 to 25 kV. The effects of the weight ratios and applied voltage on the morphology and diameter of the fibers were investigated. The resultant fibers were characterized using scanning electron microscopy (SEM), transmission electron microscopy (TEM), Fourier transform infrared spectroscopy (FTIR), X-ray diffraction (XRD), and thermogravimetric analysis (TGA). The SEM results showed that increasing the amount of chitosan in the CS/PVA blend resulted in a decrease in the fiber diameter from 162 to 89 nm while an increase in the voltage from 15 to 25 kV led to a decrease in the fiber diameters. Furthermore, the SEM results indicated that an increase in the fiber diameter from 161 to 257 nm was observed while morphological changes were also observed upon the Ag/Cu addition. The latter changes are perceived to be a result of increased conductivity and higher charge density.

1. Introduction

Electrospinning is a simple, reproducible, and cost-effective method used to produce fibers with diameters ranging from 10 micrometers (μm) to 10 nanometers (nm) [1]. It is considered the most promising method precisely due to its ability to create continuous fibers on a larger scale. The nanofibers produced by the electrospinning process have shown remarkable properties such as a high surface area to volume ratio, microporosity, and the ability to load drugs and other biomolecules into the fibers [1]. Due to these intrinsic properties, electrospun nanofibers have found considerable attention in many biomedical applications such as wound dressing, drug delivery, and scaffolds for tissue engineering [2–4]. Electrospinning of polymer blends as candidate materials for many biomedical appli-

cations has been investigated, and polymer blends were found to provide an efficient way to fulfill new requirements for material properties [5–8]. Therefore, the production of new and cost-effective materials is of great importance. Blending both the natural and synthetic polymers might help in improving the mechanical strength, durability, and cell affinity of the nanofiber scaffolds [9]. Polymers such as chitosan (CS) and poly(vinyl alcohol) (PVA) were used in this study to produce polymer blend composite nanofibers. These polymers have been chosen due to the inherent and interesting properties that they possess. CS is a linear polysaccharide composed of randomly distributed β -(1,4)-linked D-glucosamine and N-acetyl-D-glucosamine. Chitosan (CS) is a natural polymer that has good biocompatibility [10], biodegradability, cellular binding capability, antimicrobial activity, and wound

healing effect [11]. PVA is a water-soluble synthetic polymer derived from the hydrolysis of polyvinyl acetate. It has many properties such as biocompatibility, biodegradability, and nontoxicity and is known to have the ability to form good fibers [12].

The study on polymer composite nanofiber materials has received remarkable attention nowadays, and it has been proven to be of significant importance in various applications [13]. Recently, there has been a growing interest in the incorporation of inorganic nanoparticles into polymer nanofibers for antibacterial applications [14]. Silver (Ag) nanoparticles have been found to exhibit interesting antibacterial activities against a wide spectrum of microbes [15]. Previous studies have shown that Ag nanoparticles can effectively kill pathogenic bacteria such as *Staphylococcus aureus*, *Bacillus subtilis*, and *Escherichia coli* [16]. Moreover, the latter nanoparticles have also been used in various polymer materials as coatings or in composite materials for drug delivery applications [17]. Other metals such as copper (Cu) which belong in the same group as Ag but have not yet been explored that much especially in the nanofibers as composite materials exhibit similar properties as Ag. Cu nanoparticles are known to prevent the growth of fungi, algae, and bacteria effectively and display a broad-spectrum biocide [18]. These nanoparticles exhibit unique properties such as good conductivity, chemical stability, and antimicrobial activity [19]. In this study, both the Ag and Cu nanoparticles were synthesized and incorporated into the polymer blends with a view to producing a polymer blend composite nanofiber material for wound healing applications. The composite nanofibers containing Ag nanoparticles with various polymers such as gelatin, poly(vinyl alcohol), chitosan, and poly(ethylene oxide) have been reported before. However, to the best of our knowledge, no study on the fabrication and characterization of Ag/Cu-incorporated CS/PVA blend composite fibers is found in the literature.

2. Experimental Section

2.1. Materials. The materials used in the study include the following: silver nitrate (AgNO_3) (99%) analytical reagent (AR) grade, cupric oxalate, oleylamine technical grade 70%, ethanol, toluene, chitosan (medium molecular weight), poly(vinyl alcohol) (PVA; $M_w = 89,000 - 98,000$, 99+% hydrolyzed), acetic acid 98%, and distilled water. All chemicals were purchased from Sigma-Aldrich and used without purification.

2.2. Instrumentation

2.2.1. Optical Characterization. The optical measurements were carried out using a PerkinElmer Lambda 25 UV/Vis spectrophotometer (ELICO-SL-150). The samples were placed in quartz cuvettes (1 cm path length) using ethanol and toluene as reference solvents for copper and silver, respectively. The samples were scanned from 900 to 200 nm in order to find the maximum absorbance and surface plasmon resonance (SPR) of Ag and Cu nanoparticles.

TABLE 1: Variation of precursor concentrations in 6 mL of oleylamine.

Sample	Concentration in g/6 mL of oleylamine	Temperature (°C)
1	0.1	180
2	0.15	180
3	0.2	180

2.2.2. Transmission Electron Microscopy (TEM). The TEM images were recorded using a Hitachi JEOL 100S transmission microscope operating at 80 kV. The nanoparticles were diluted in toluene, and a droplet of a solution was placed on a carbon-coated copper grid. The samples were dried at room temperature prior to analysis.

2.2.3. Scanning Electron Microscopy (SEM). The FE-SEM (LEO Zeiss) scanning electron microscope operated at 1.00 kV, and the electron potential difference was used to study the morphology and diameter of the fibers. The fibers were carbon-coated prior to analysis.

2.2.4. X-Ray Diffraction (XRD). The powder X-ray diffraction patterns of the nanoparticles were recorded by a Bruker D2 diffractometer operating at 40 kV/30 mA using secondary graphite monochromated $\text{Co K}\alpha$ radiation ($\lambda = 1.7902$). Measurements were taken at a high-angle 2θ range of $5-90^\circ$ with a scan step of 0.01° . The fibers and the composite fibers were recorded by a Shimadzu XRD-7000 X-ray diffractometer at 40 kV/30 mA using secondary graphite monochromated $\text{Cu K}\alpha$ radiation ($\lambda = 1.7902$). Measurements were taken at a high-angle 2θ range of $10-80^\circ$ with a scan speed of 2 degrees/minute ($2^\circ/\text{min}$) and a scan step of 0.02° .

2.2.5. FTIR Spectrometry. FTIR spectra of the fibers and the composite fibers were recorded using a Nicolet iS50 FTIR spectrometer ranging from 400 to 4000 cm^{-1} . The samples were placed onto the universal ATR sample holder and pressed on top by a gauge force arm.

2.2.6. Thermogravimetric Analysis (TGA). Thermogravimetric analysis of the fibers and the composite fibers was performed using a PerkinElmer TGA 4000 thermal analyzer under nitrogen with a flow rate of $20^\circ\text{C}/\text{min}$. The samples were heated from 30 to 800°C at a heating rate of $10^\circ\text{C}/\text{min}$.

2.3. Preparation of Nanoparticles

2.3.1. Synthesis of Ag and Cu Nanoparticles. This method for the synthesis of silver (Ag) and copper (Cu) nanoparticles was adopted from Chen et al. [20] with minor modification. In a typical experiment, 0.1-0.2 g of AgNO_3 was added to 6 mL of oleylamine. The solution was then transferred into a three-neck round-bottom flask and refluxed for 1 hr under the flow of nitrogen gas at 180°C . After 1 hr, the reaction was stopped and cooled to about 70°C . The Ag nanoparticles formed were precipitated with excess ethanol and then separated by centrifugation at 12,000 rpm for 10 min. The particles were washed three times with ethanol to remove excess

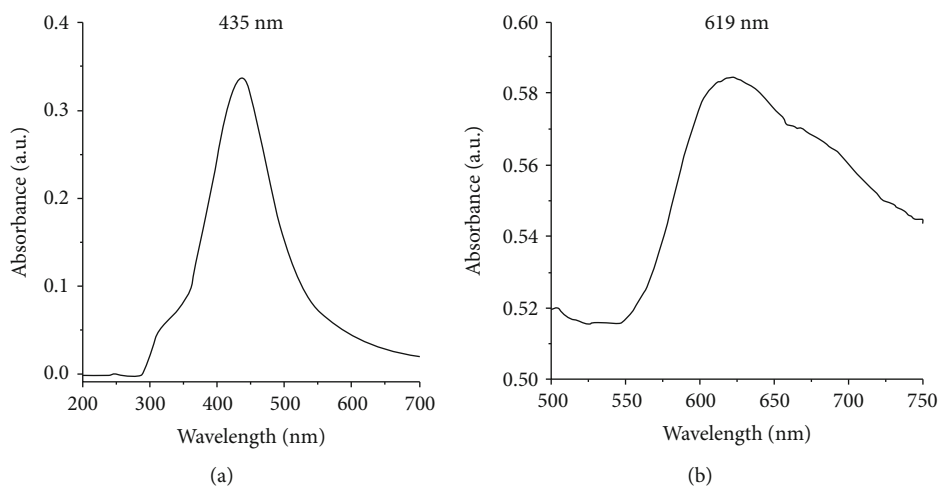


FIGURE 1: Absorption spectra of oleylamine-capped Ag (a) and Cu (b) nanoparticles prepared using 0.15 g precursor concentration.

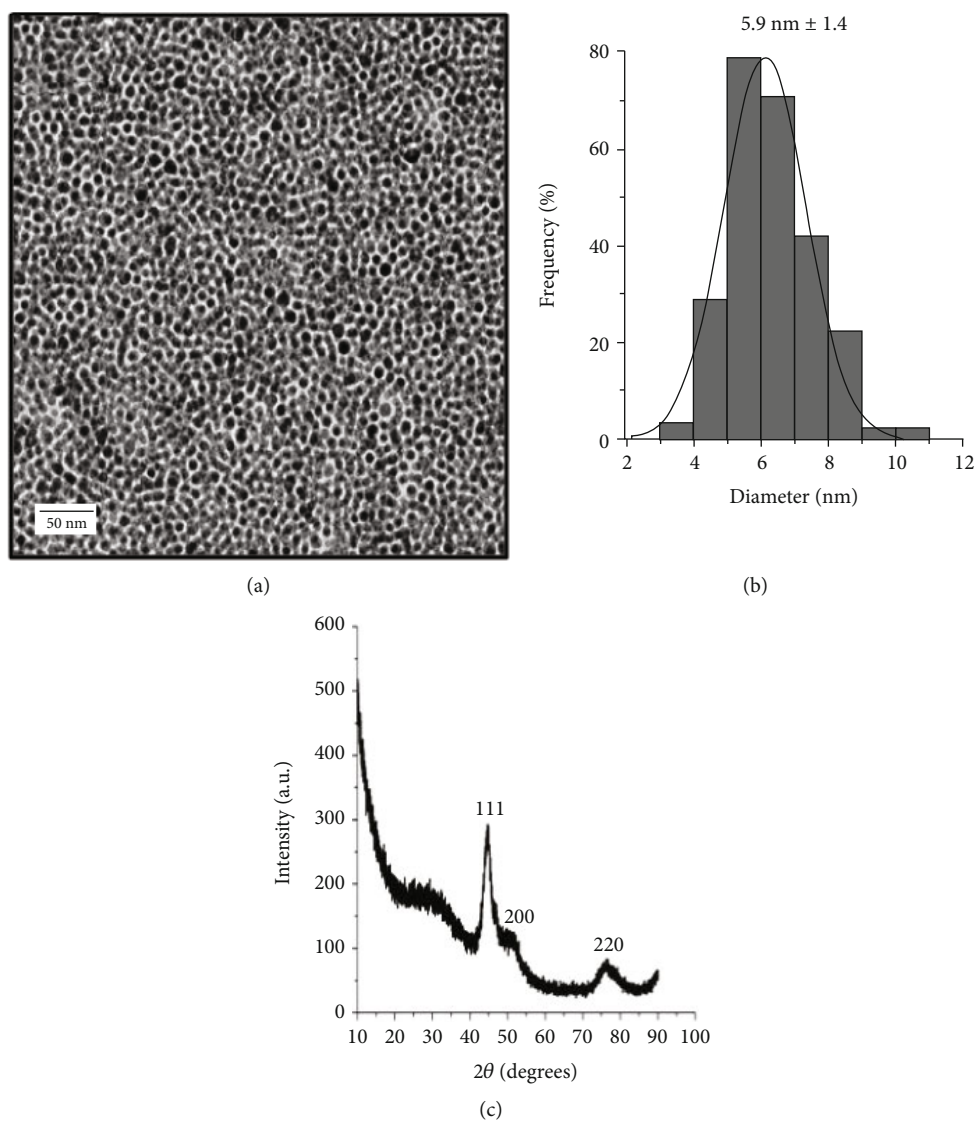


FIGURE 2: TEM image (a), size distribution (b), and XRD patterns (c) of Ag nanoparticles.

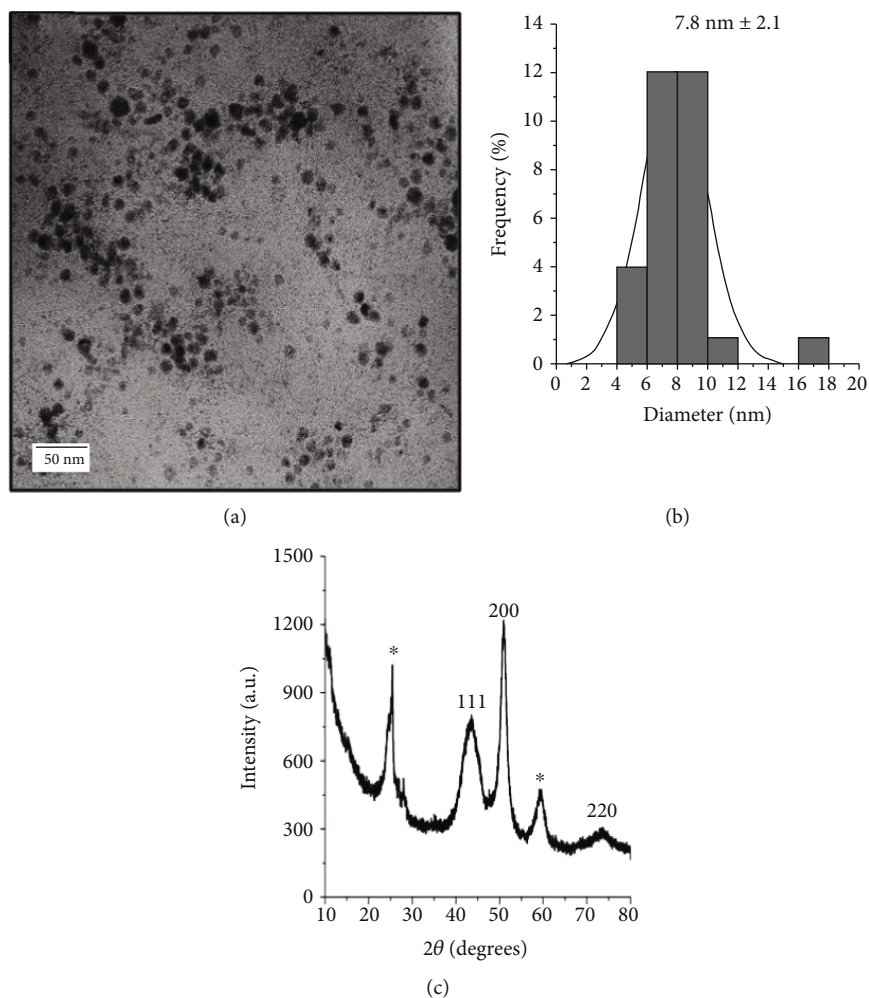


FIGURE 3: TEM image (a), size distribution (b), and XRD patterns (c) of Cu nanoparticles.

oleylamine. The resulting nanoparticles were left to dry for further characterization. The same procedure was used for the synthesis of Cu nanoparticles using cupric oxalate as a precursor. The growth of Ag and Cu nanoparticles was studied by varying the effect of precursor concentration from 0.1 to 0.2 g for both the Ag and Cu nanoparticles. All the precursor concentrations in g/6 mL of oleylamine are shown in Table 1.

2.3.2. Preparation of CS/PVA Blend Ratios and Ag/Cu/CS/PVA Composite Nanofibers. Blend solutions were prepared by making separately 2 wt% chitosan solution in acetic acid and 16 wt% PVA solution using water as the solvent. The two solutions were subsequently mixed in the weight ratios of 20/80, 30/70, 40/60, and 50/50 of CS/PVA, respectively. Different amounts of Ag/Cu nanoparticles ranging from 0.1 to 0.4 wt% were added directly to PVA solutions and stirred for 1 hr for complete dispersion. After 1 hr, the prepared solutions were transferred to the CS solutions and stirred further for 2 hrs. The mixed solutions were then subjected to electrospinning, and the polymer solution was placed in a 20 mL plastic syringe fitted with a stainless steel needle of tip dimensions of 1.20×38 mm. The outer diame-

ter of the needle was 1.270 mm, and the inner diameter was 0.838 mm with an 18-gauge needle. A high voltage power supply was used to produce the voltages ranging from 15 to 25 kV, and the distance between the nozzle and the collector screen was kept at 15 cm with a flow rate of 0.050 mm/min. The addition of Ag/Cu nanoparticles was effective only under the condition of a 30/70 weight ratio (CS/PVA), with a voltage of 20 kV, a spinning distance of 15 cm, and a flow rate of 0.05 mm/min.

3. Results and Discussion

Ag and Cu nanoparticles were synthesized using the thermal decomposition method in the presence of oleylamine as a capping agent. This method is well known to produce good stable uniform monodispersed nanoparticles. The 0.15 g concentration was chosen as the optimum concentration for both the Ag and Cu nanoparticles because of their uniformity and spherical shape. The average size diameter was found to be 5.9 nm for Ag and 7.8 nm for Cu nanoparticles. The as-prepared Ag and Cu nanoparticles were further incorporated into the CS/PVA polymer blend. The effects of the weight ratio, voltage, and Ag/Cu nanoparticle loading on the

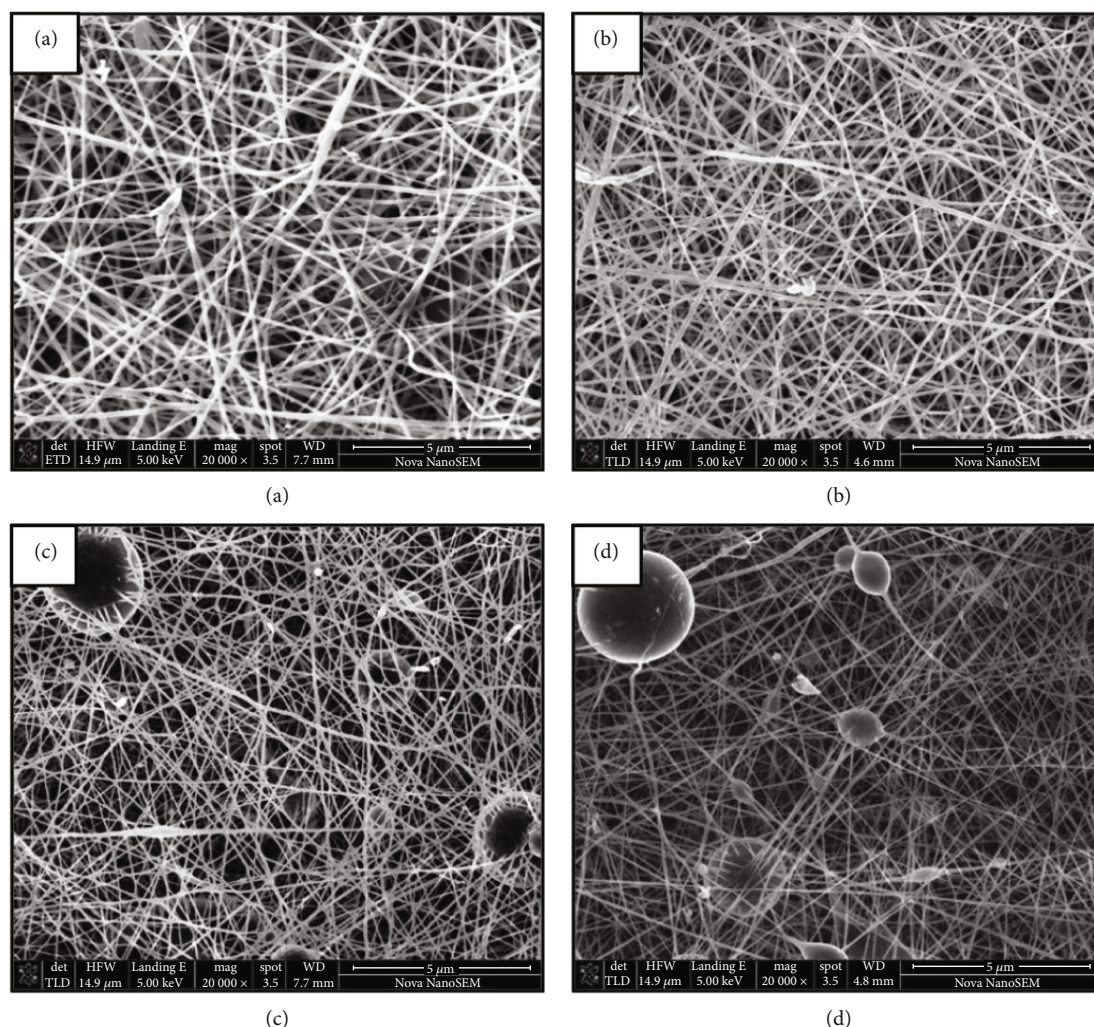


FIGURE 4: SEM images of electrospun nanofibers prepared with different weight ratios of (a) 20/80, (b) 30/70, (c) 40/60, and (d) 50/50 of CS/PVA at a voltage of 15 kV and a distance of 15 cm.

morphology and diameter of the fibers were investigated in this study.

3.1. Synthesis and Characterization of Ag and Cu Nanoparticles

3.1.1. Optical Properties of Silver and Copper Nanoparticles.

Metal nanoparticles such as Ag, Cu, and gold (Au) show a distinct surface plasmon resonance (SPR) in the visible region [21]. This SPR band is sensitive to the metal size, embedding medium, and dielectric constant of the metal [22, 23]. The formation of Ag and Cu nanoparticles was observed using UV-Vis absorption spectroscopy. The absorption spectrum of silver nanoparticles in Figure 1(a) showed the surface plasmon band at 435 nm which indicates the presence of spherical Ag nanoparticles. Figure 1(b) shows a broad absorption peak at 619 nm that is assigned to the SPR band of Cu nanoparticles. This broadness of the absorption band could be attributed to the wide size distribution of Cu nanoparticles. It has been reported in the literature that the SPR band of Cu nanoparticles appears in the range of 350-800 nm, as the exact SPR band is not known [24, 25]. Both

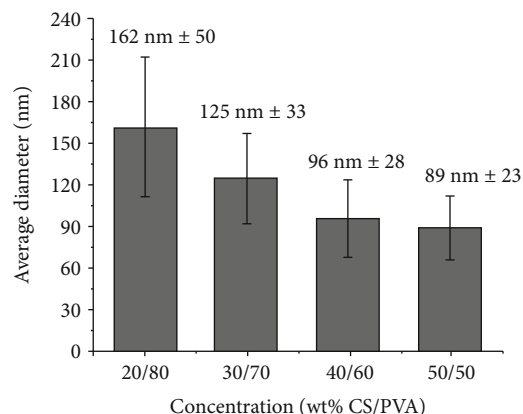


FIGURE 5: Average diameter of the electrospun CS/PVA nanofibers at different weight ratios (voltage 15 kV, distance 15 cm).

the Ag and Cu nanoparticles showed a blueshift from their bulk materials with the bulk values of 1000 nm for Ag and 1100 nm for Cu nanoparticles.

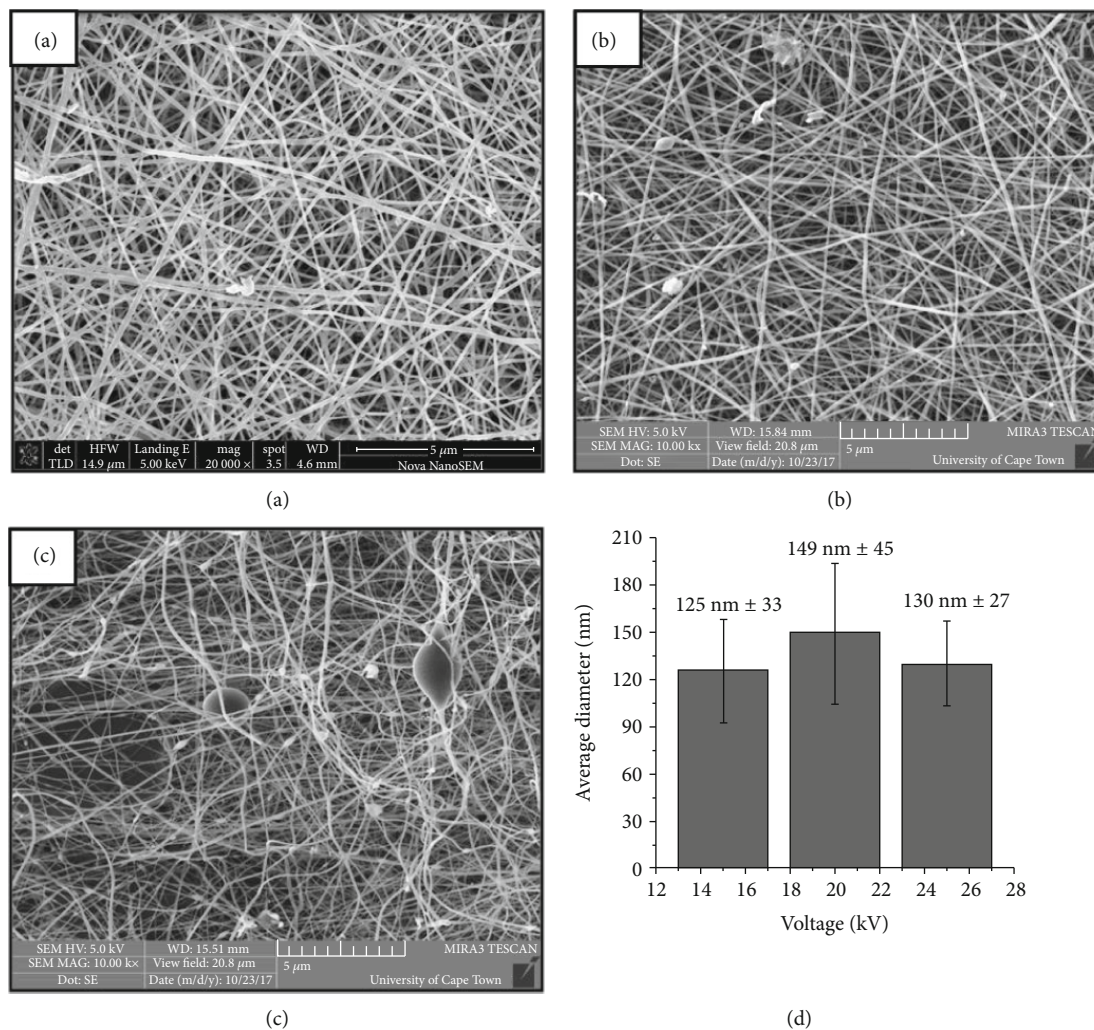


FIGURE 6: SEM images and average fiber distribution of the 30/70 CS/PVA blend at different voltages of (a) 15 kV, (b) 20 kV, and (c) 25 kV with a spinning distance of 15 cm.

3.1.2. Structural Characterization of Silver and Copper Nanoparticles. Figures 2(a)–2(c) show the TEM image, size distribution, and XRD pattern of Ag nanoparticles prepared at a precursor concentration of 0.15 g/6 mL of oleylamine. Figure 2(a) shows that uniform, monodispersed, and spherical particles were observed with an average particle size of 5.9 nm, as shown by the size distribution in Figure 2(b). The crystal structure of Ag nanoparticles was further characterized with X-ray diffraction shown in Figure 2(c). All diffraction peaks at $2\theta = 44.3^\circ$, 51.3° , and 76.0° correspond to (111), (200), and (220) planes which were identified as Ag in the face-centered cubic (fcc) (JCPDS, 03-065-2871).

The TEM image, size distribution, and XRD pattern of Cu nanoparticles are shown in Figures 3(a)–3(c), respectively. The TEM image of Cu nanoparticles shows uniform and spherical particles with an average diameter of 7.8 nm, as confirmed by the size distribution graph in Figure 3(b). The XRD pattern of Cu nanoparticles shows peaks at $2\theta = 43.5^\circ$, 50.7° , and 74.0° corresponding to (111), (200), and (220) planes which suggest Cu in the face-centered cubic (fcc) structure. Some pieces of evidence of impurities were

also observed indicating the presence of Cu_2O in the sample due to oxidation in air.

3.2. Electrospinning of Ag/Cu Nanoparticle-Loaded CS/PVA Blended Nanofibers. Polymer blends are a mixture of two chemically different polymers combined in sum arbitrary proportion. CS and PVA solutions were mixed and electrospun to produce polymer blend nanofibers with improved physicochemical properties. The electrospinning of CS solution was more challenging due to its high viscosity and polycationic character mainly caused by many amino groups found in its backbone. The latter properties are believed to be the reasons for the increased surface tension of the solution. Hence, a strong electrical force is needed to overcome the high surface tension in order to produce CS nanofiber mats. However, more particles were often formed during the electrospinning process which might be due to the force of repulsion that occurs between the ionic groups of CS in acidic aqueous solution [26]. Therefore, the addition of PVA solution into chitosan solution improved the electrospinnability of the CS solution. The morphology and

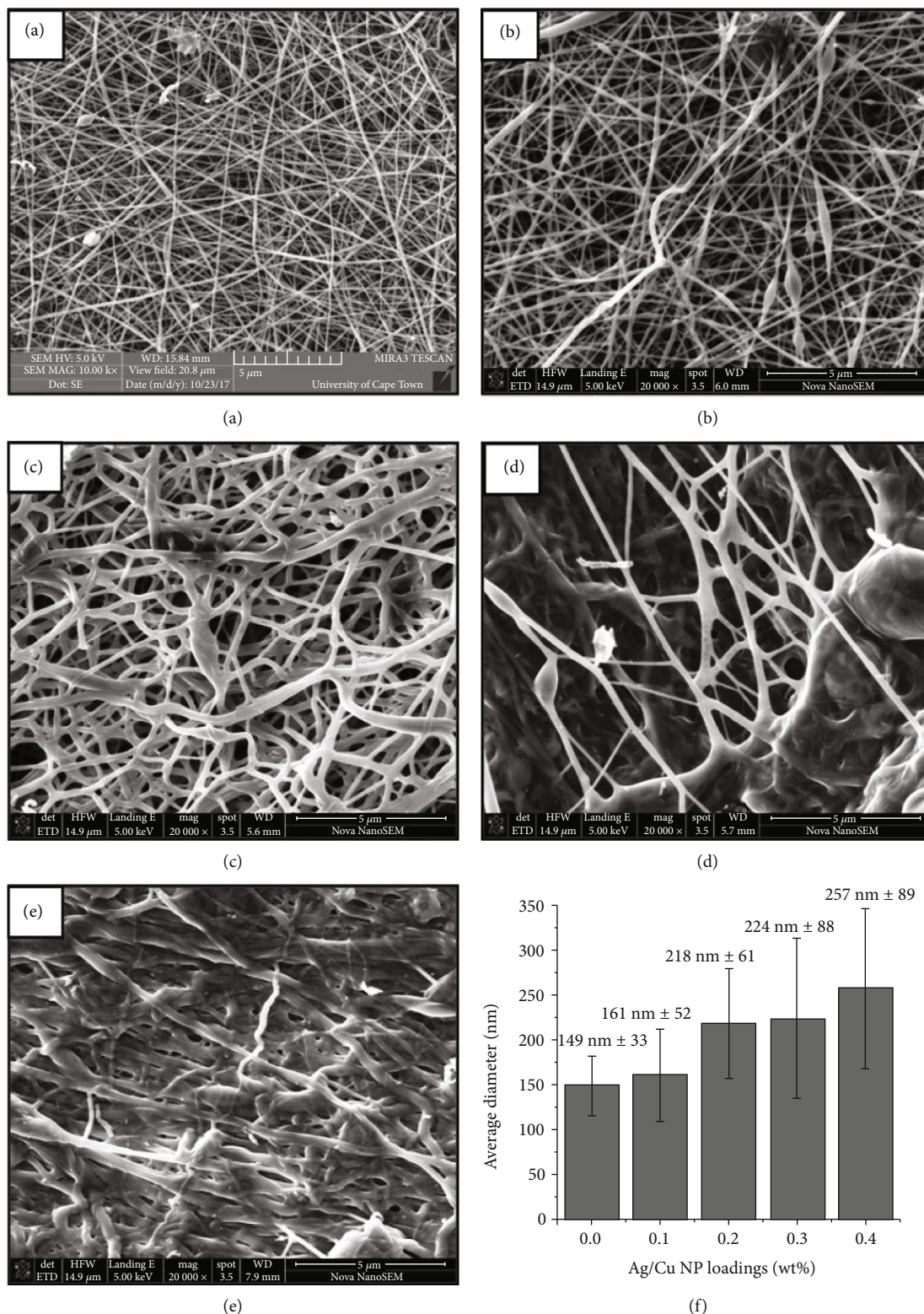


FIGURE 7: SEM images and fiber distribution of the 30/70 CS/PVA blend with different Ag/Cu nanoparticle loadings of (a) 0 wt%, (b) 0.1 wt%, (c) 0.2 wt%, (d) 0.3 wt%, and (e) 0.4 wt%. Voltage: 20 kV; distance: 15 cm.

diameter of the blend fibers were investigated by varying the effect of the weight ratio, voltage, and loading of a mixture of Ag/Cu nanoparticles into the fibers.

3.2.1. *Effect of Weight Ratios on the Morphology of the Nanofibers.* The SEM images and average fiber distribution of the electrospun CS/PVA blend with different weight ratios

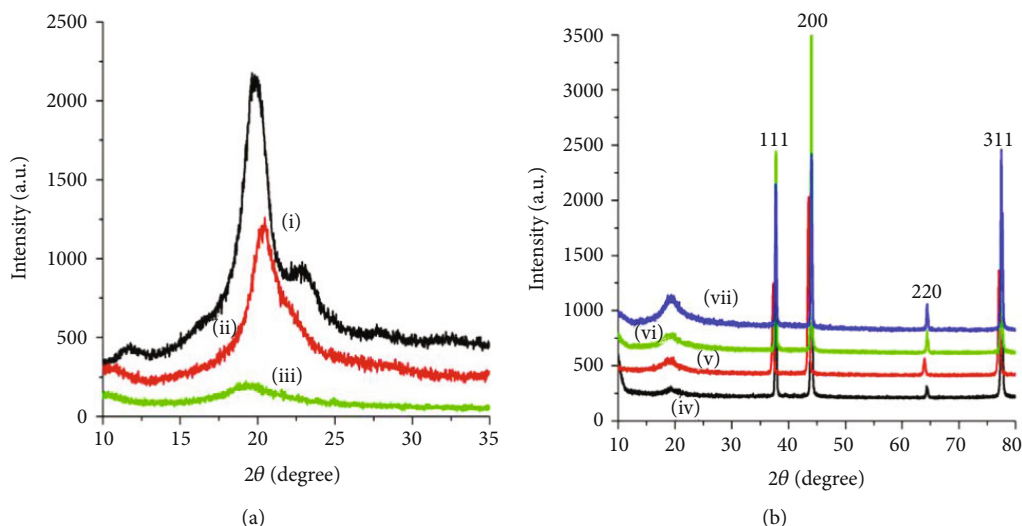


FIGURE 8: XRD pattern spectra of the (a) (i) pure PVA, (ii) pure CS, (iii) 30/70 CS/PVA blend, and (b) (iv) 0.1 wt%, (v) 0.2 wt%, (vi) 0.3 wt%, and (vii) 0.4 wt% Ag/Cu/CS/PVA. Voltage: 20 kV; distance: 15 cm.

of CS/PVA are shown in Figures 4(a)–4(d). The fiber diameters decreased continuously at ratios ranging from 20/80 to 50/50, and this could be due to the increased amount of chitosan in the blend. The average fiber diameters were found to be 162, 125, 96, and 89 nm for 20/80, 30/70, 40/60, and 50/50, respectively, and this was observed from the fiber distribution graph in Figure 5. Uniform fibers were only observed from the blend ratios of 20/80 and 30/70. When the blend ratio was increased to 40/60, fewer beads with fibers were observed. Thin fibers with more beads were observed at the blend ratio of 50/50, and this could be due to the high charge density that is formed on the surface of the jet which in turn causes the forces of elongation to be imposed on the jet under the electrical field resulting in decreased fiber diameters. These results are in agreement with the previous study done by Jia and coworkers on the effect of weight ratios on the morphology and diameter of the fibers using the CS/PVA blend, and they demonstrated that increasing the amount of chitosan in the blend from 10 to 30% resulted in a gradual decrease in the average fiber diameter [12]. They further mention that above 30% fibers could hardly be formed due to the fact that chitosan is an ionic polyelectrolyte, and higher charge density on the surface of the jet is formed during electrospinning which prevented the formation of continuous fibers.

3.2.2. Effect of Applied Voltages on the Morphology and Diameter of the Fibers. Electrospinning is governed by many parameters that influence the formation of fibers. The applied voltage is one of those parameters that affect the electrospinning process. Yordem et al. [27] have reported that the applied voltage influences the fiber diameter, but its level of significance varies with the polymer concentration and on the distance between the tip and the collector. The effect of the applied voltage on the morphology and diameter of the fibers was investigated using SEM. Figures 6(a)–6(d) show the SEM images and average fiber diameters of CS/PVA nanofibers at different voltages ranging from 15 to 25 kV.

The optimum blend ratio of 30/70 CS/PVA was used at a fixed nozzle-to-collector distance of 15 cm. The SEM results of the electrospun nanofibers showed that uniform morphologies and an increase in fiber diameters from 125 to 149 nm were observed at voltages 15 and 20 kV. This could be a result of the stability of the jet caused by increased charge density on the surface of the jet, polymer strand elongation forces, and polymer jet velocity [28]. When the voltage was further increased to 25 kV, a mixture of beads and fibers was observed with the average fiber diameter decreasing to 130 nm. This is as a result of an increase in the electric field strength which resulted in an increase in the electrostatic repulsive force on the fluid jet, thus favoring thinner fiber diameters.

3.2.3. Effect of Nanoparticle Loadings on the Morphology of the Fibers. In electrospinning, inorganic salts may be added to a polymer solution to influence its viscosity, surface tension, and conductivity. Since solution conductivity has a major influence on the process, the effect of Ag/Cu nanoparticles loaded on the morphology and diameter of the fibers was investigated. Zong et al. [29] have studied the effect of ions on the morphology and diameter of the electrospun fibers, and they found that the addition of ionic salts to the polymer solution produced beadless fibers with reduced diameters. It has also been known that the addition of ionic salts in the polymer solution can increase the conductivity of the solution and thereby increase the charge density on the surface of the ejected jet resulting in particles like beads being formed during electrospinning.

Figures 7(a)–7(f) show the SEM images and average fiber diameter of the pure 30/70 CS/PVA blend and Ag/Cu/CS/PVA nanocomposite fibers with different nanoparticle loadings ranging from 0.1 to 0.4 wt% at a voltage of 20 kV and a distance of 15 cm. The 30/70 CS/PVA blend showed uniform fibers with a smaller fiber diameter. However, the addition of Ag/Cu nanoparticles into the 30/70 CS/PVA blend ratio resulted in a significant increase in the

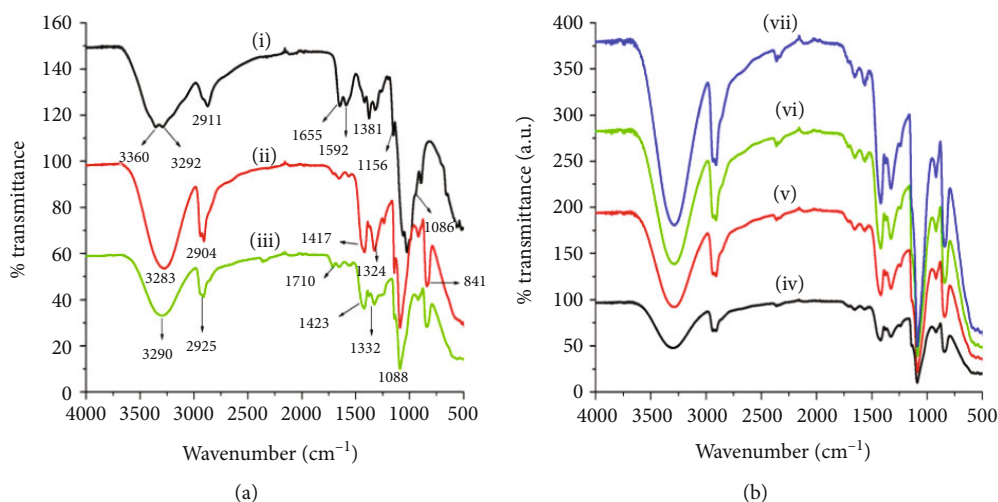


FIGURE 9: FTIR spectra of the (a) (i) pure chitosan, (ii) pure PVA, (iii) 30/70 CS/PVA blend, and (b) (iv) 0.1 wt%, (v) 0.2 wt%, (vi) 0.3 wt%, and (vii) 0.4 wt% Ag/Cu/CS/PVA. Voltage: 20 kV; distance: 15 cm.

average fiber diameter of 161, 218, 224, and 257 nm for 0.1, 0.2, 0.3, and 0.4 wt%, respectively, with irregular morphologies.

Uniform fibers with fewer beads were also observed for 0.1 wt% Ag/Cu/CS/PVA composite fibers. When the concentration of Ag/Cu nanoparticles was increased from 0.2 to 0.4 wt% in the CS/PVA blend, the uniformity of the nanofibers changed and some defects such as branched fibers, bead-like structures, and ribbons were observed. This change in uniformity at higher loadings could be a result of increased conductivity and viscosity of the solution.

The XRD analysis of the electrospun CS/PVA blend and its composite fibers was performed to investigate the structural properties and the influence of the nanoparticle loading on the structure of the polymer blend. Figure 8(a) shows the XRD patterns of (i) pure PVA, (ii) pure CS, (iii) CS/PVA blend nanofibers, and Ag/Cu/CS/PVA composite fibers at different concentrations (0.1–0.4 wt%). There are three diffraction peaks observed for pure PVA at $2\theta = 11.7^\circ$, 19.6° , and 22.9° . For pure CS, two peaks around $2\theta = 10.5^\circ$ and 20.4° were observed. This broad peak for both CS and PVA shows the amorphous nature of the polymers. For CS/PVA blend nanofibers, there is a broad peak around $2\theta = 19.4^\circ$. The peak observed for CS at $2\theta = 10.5^\circ$ disappeared and might be due to the intermolecular hydrogen bonding that occurs when CS and PVA are blended together. The PVA peaks at $2\theta = 11.7$ and 22.9 also disappeared with increasing CS content in the blend due to intermolecular hydrogen bonding between CS/PVA blends. The composite fibers in Figure 8(b) (iv–vii) showed four diffraction peaks at $2\theta = 37.7^\circ$, 44.1° , 64.5° , and 77.5° , and they were assigned to (111), (200), (220), and (311) planes, respectively, suggesting the presence of Ag nanoparticles in the face-centered cubic (fcc). The results from the composite show that crystalline peaks of Ag nanoparticles in this material are the most dominant than those of Cu nanoparticles, and this could be due to the high conductivity of silver in the solution. Another reason might be that Cu is smaller than silver and it can easily

dissolve in the Ag matrix causing lattice contraction [30]. The calculated sizes of Cu and Ag are 128 and 144 pm, respectively. The peak around $2\theta = 19.4^\circ$ was observed for all the composite fibers which proves that there is a complete interaction between CS and PVA.

3.3. Material Characterization

3.3.1. FTIR Spectrometry. The FTIR spectral analysis was used to determine the structural functionality of the polymers and also check if there was any chemical interaction between the blend nanofibers and the mixture of nanoparticles. Figure 9 shows the FTIR spectra of the pure chitosan, pure PVA, CS/PVA blend, and Ag/Cu/CS/PVA composite fibers. For pure CS, the broad band in the region of 3360 cm^{-1} – 3293 cm^{-1} corresponds to O-H and N-H stretching vibrations with intermolecular hydrogen bonds overlapping inside the broad absorption band. The peak assigned to the C-H stretching vibration was observed at 2911 cm^{-1} . The peaks at 1655 cm^{-1} and 1592 cm^{-1} correspond to the amide I (C=O stretching) and amide II (N-H bending) vibrations. The peaks at 1381 cm^{-1} and 1318 cm^{-1} were attributed to the CH_3 symmetrical deformation and amide III (C-N stretching). The band at 1156 cm^{-1} may be due to the asymmetric stretching vibration of the C-O-C bridge, and the sharp peak at 1030 cm^{-1} corresponds to the C-O stretching vibration of the chitosan polymer. For pure PVA, the broad absorption peak assigned to the O-H stretching vibration was observed at 3283 cm^{-1} and the peak at 2904 cm^{-1} corresponds to the C-H stretching vibration. The peak at 1662 cm^{-1} corresponds to the C=O stretching vibration of nonhydrolyzed vinyl acetate groups in PVA. The peaks at 1417 cm^{-1} and 1324 cm^{-1} are assigned to the CH_3 stretching and deformation. The same peak at 1086 cm^{-1} occurs for both CS and PVA and is due to the C-O bending and stretching vibration. Additionally, comparing the FTIR spectra of PVA and CS, the peak assigned to the C-H bending vibration for PVA was observed at 841 cm^{-1} and was not detected in CS. This

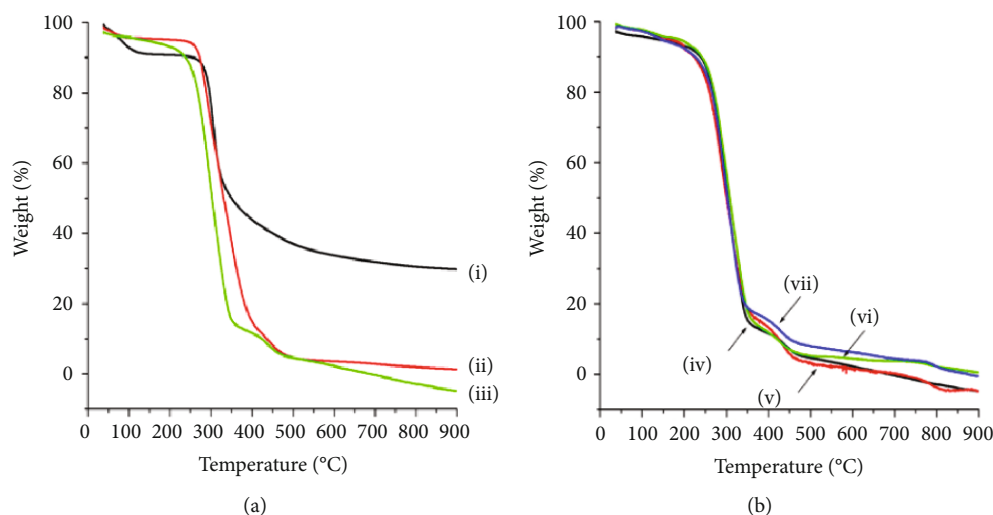


FIGURE 10: TGA curves of the (a) (i) pure PVA, (ii) pure CS, (iii) 30/70 CS/PVA blend, and (b) (iv) 0.1 wt%, (v) 0.2 wt%, (vi) 0.3 wt%, and (vii) 0.4 wt% Ag/Cu/CS/PVA. Voltage: 20 kV; distance: 15 cm.

result does suggest the formation of intermolecular hydrogen bonds between the CS and PVA molecules. However, the absorption peak found around 841 cm^{-1} for PVA also appeared in the spectrum of the CS/PVA blend. For the CS/PVA blend, the absorption bands at 1655 cm^{-1} and 1592 cm^{-1} disappeared due to the loss of free amine in the compound. The FTIR spectra of the composite fibers at different concentrations gave almost identical features as the blend, with the CS bands at 1156 cm^{-1} , 1655 cm^{-1} , and 1592 cm^{-1} disappearing in both the blend and the composites which indicates the formation of hydrogen bonds between the two polymers. An increase in the intensity of the C-H group was observed for the composite fibers when the mixture of Ag/Cu nanoparticles was increased.

3.3.2. Thermogravimetric Analysis (TGA). The TGA was carried out to investigate the thermal stability of the polymers and the effect of nanoparticle loading on the thermal stability of the blends. Figure 10 shows the TGA graphs of the pure CS, pure PVA, CS/PVA blend, and composite fibers. Chitosan undergoes three decomposition stages. The first decomposition stage occurred between 38°C and 100°C , and this was due to the loss of moisture in the sample with 10% weight loss. The second stage between 135°C and 233°C was due to the primary degradation of chitosan, and the last stage which resulted in the degradation of polysaccharides and decomposition of chitosan main chains was from 233°C to 400°C with a weight loss of 52%. TGA graph of the PVA polymer shows three decomposition stages with the first stage occurring between 38° and 100°C due to moisture vaporization. The decomposition step of the PVA side chain for the second stage occurred around 243°C . The third stage between 400°C and 500°C was due to the loss of the PVA main chain (nonhydrolyzed vinyl acetate group) with a weight loss of 6%. The thermal stability of the CS/PVA blend seemed lower as compared to that of the pure polymers. It is apparent that the nanoparticle loadings did not have an influence on the thermal stability of the composite fibers.

4. Conclusion

Oleylamine-capped Ag and Cu nanoparticles were prepared using the thermal decomposition method. TEM results showed that uniform and spherical shape nanoparticles were observed with a small average size. The XRD results show peaks which were identified as Ag and Cu in the face-centered cubic. The absorption maxima of Ag and Cu nanoparticles showed a blueshift from the bulk material. SEM images of the CS/PVA blends at different weight ratios showed that the fiber diameters decreased with an increased amount of chitosan in the blend resulting in the formation of a mixture of beads and fibers. The increase in the applied voltage seemed to have affected both morphologies and fiber diameters. The addition of Ag and Cu nanoparticles in the blend resulted in an increase in the average fiber diameters and an irregular fiber morphology. The XRD patterns of the CS, PVA, and CS/PVA blend showed the amorphous broad peaks for both polymers and blends whereas the composite fibers showed peaks which corresponded to Ag in the face-centered cubic phase. In this case, Ag peaks seemed to be the dominant ones as compared to the Cu nanoparticles. The XRD data further indicated that Ag/Cu nanoparticles were successfully incorporated into the polymer nanofibers. The FTIR results showed some interactions between the polymers and the nanoparticles. The thermal stability of the composite fibers was not influenced by the nanoparticle loadings.

Data Availability

Data for the manuscript have been provided within the text, but if additional information is required, data can be made available upon request.

Conflicts of Interest

The authors would like to declare no conflict of interest of any form with regard to the work presented in this manuscript.

Acknowledgments

The authors would like to thank Vaal University of Technology, Chemistry Department, for lab space and funding. Thanks are also due to Mintek for using their electrospinning technique.

References

- [1] M. Abrigo, S. L. McArthur, and P. Kingshott, "Electrospun nanofibers as dressings for chronic wound care: advances, challenges, and future prospects," *Macromolecular Bioscience*, vol. 14, no. 6, pp. 772–792, 2014.
- [2] B. M. Min, G. Lee, S. H. Kim, Y. S. Nam, T. S. Lee, and W. H. Park, "Electrospinning of silk fibroin nanofibers and its effect on the adhesion and spreading of normal human keratinocytes and fibroblasts in vitro," *Biomaterials*, vol. 25, no. 7-8, pp. 1289–1297, 2004.
- [3] J. A. Matthews, G. E. Wnek, D. G. Simpson, and G. L. Bowlin, "Electrospinning of collagen nanofibers," *Biomacromolecules*, vol. 3, no. 2, pp. 232–238, 2002.
- [4] W. J. Li, C. T. Laurencin, E. J. Caterson, R. S. Tuan, and F. K. Ko, "Electrospun nanofibrous structure: a novel scaffold for tissue engineering," *Journal of Biomedical Materials Research*, vol. 60, no. 4, pp. 613–621, 2002.
- [5] C. J. Sajitha and D. Mohan, "Studies on cellulose acetate-carboxylated polysulfone blend ultrafiltration membranes?Part II," *Polymer International*, vol. 52, no. 1, pp. 138–145, 2003.
- [6] E. R. Kenawy, G. L. Bowlin, K. MansWeld et al., "Release of tetracycline hydrochloride from electrospun poly(ethylene-co-vinylacetate), poly(lactic acid), and a blend," *Journal of Controlled Release*, vol. 81, no. 1-2, pp. 57–64, 2002.
- [7] B. M. Min, Y. You, J. M. Kim, S. J. Lee, and W. H. Park, "Formation of nanostructured poly(lactic-co-glycolic acid)/chitin matrix and its cellular response to normal human keratinocytes and fibroblasts," *Carbohydrate Polymer*, vol. 57, no. 3, pp. 285–292, 2004.
- [8] Y. You, S. W. Lee, J. H. Youk, B. M. Min, S. J. Lee, and W. H. Park, "In vitro degradation behaviour of non-porous ultra-fine poly(glycolic acid)/poly(l-lactic acid) fibres and porous ultra-fine poly(glycolic acid) fibres," *Polymer Degradation and Stability*, vol. 90, no. 3, pp. 441–448, 2005.
- [9] N. Bhardwaj and S. C. Kundu, "Electrospinning: a fascinating fiber fabrication technique," *Biotechnology Advances*, vol. 28, no. 3, pp. 325–347, 2010.
- [10] S. B. Rao and C. P. Sharma, "Use of chitosan as a biomaterial: studies on its safety and hemostatic potential," *Journal of Biomedical Materials Research*, vol. 34, no. 1, pp. 21–28, 1997.
- [11] M. Rinaudo, "Chitin and chitosan: properties and applications," *Progress in Polymer Science*, vol. 31, no. 7, pp. 603–632, 2006.
- [12] Y.-T. Jia, J. Gong, X.-H. Gu, H.-Y. Kim, J. Dong, and X.-Y. Shen, "Fabrication and characterization of poly(vinyl alcohol)/chitosan blend nanofibers produced by electrospinning method," *Carbohydrate Polymers*, vol. 67, no. 3, pp. 403–409, 2007.
- [13] B. Y. Lim, C. S. Poh, C. H. Voon, and H. Salmah, "Rheological and thermal study of chitosan filled thermoplastic elastomer composites," *Applied Mechanics and Materials*, vol. 754-755, no. 34-38, pp. 34–38, 2015.
- [14] K. T. Shalumon, K. H. Anulekha, S. V. Nair, S. V. Nair, K. P. Chennazhi, and R. Jayakumar, "Sodium alginate/poly(vinyl alcohol)/nano ZnO composite nanofibers for antibacterial wound dressings," *International Journal of Biological Macromolecules*, vol. 49, no. 3, pp. 247–254, 2011.
- [15] P. Dubey, B. Bhushan, A. Sachdev, I. Matai, S. Uday Kumar, and P. Gopinath, "Silver-nanoparticle-incorporated composite nanofibers for potential wound-dressing applications," *Journal of Applied Polymer Science*, vol. 132, no. 35, 2015.
- [16] A. V. Vishnevsky, "Silver nanoparticles electromagnetic behavior in a blood vessel," *Journal of Education*, vol. 4, no. 26, 2010.
- [17] P. Rujitanaroj, N. Pimpha, and P. Supaphol, "Preparation, characterization and anti-bacterial properties of electrospun polyacrylonitrile fibrous membranes containing silver nanoparticles," *Journal of Applied Polymer Science*, vol. 116, no. 1967-1976, 2010.
- [18] R. Ramli, M. R. Khan, N. K. Chowdhury et al., "Development of Cu nanoparticle loaded oil palm fibre reinforced nanocomposite," *Scientific Research*, vol. 2, no. 4, pp. 358–365, 2013.
- [19] U. T. Khattoon, G. V. S. Rao, and M. K. Mohan, "Synthesis and characterization of copper nanoparticles by chemical reduction method," in *International Conference on Advanced Nanomaterials & Emerging Engineering Technologies*, Chennai, India, July 2013.
- [20] M. Chen, Y.-G. Feng, X. Wang, T.-C. Li, J.-Y. Zhang, and D.-J. Qian, "Silver nanoparticles capped by oleylamine: formation, growth and self-organization," *Langmuir*, vol. 23, no. 10, pp. 5296–5304, 2007.
- [21] M. Salavati-Niasari, F. Davar, and N. Mir, "Synthesis and characterization of metallic copper nanoparticles via thermal decomposition," *Polyhedron*, vol. 27, no. 17, pp. 3514–3518, 2008.
- [22] S. Chen and J. M. Sommers, "Alkanethiolate-protected copper nanoparticles: spectroscopy, electrochemistry, and solid-state morphological evolution," *Journal of Physical Chemistry B*, vol. 105, no. 37, pp. 8816–8820, 2001.
- [23] N. A. Dhas, C. P. Raj, and A. Gedanken, "Synthesis, characterization, and properties of metallic copper nanoparticles," *Chemistry of Materials*, vol. 10, no. 5, pp. 1446–1452, 1998.
- [24] M. K. Niranjana and J. Chakraborty, "Synthesis of oxidation resistant copper nanoparticles in aqueous phase and efficient phase transfer of particles using alkanethiol," *Colloids and Surfaces A: Physicochemical and Engineering Aspects*, vol. 407, pp. 58–63, 2012.
- [25] X. Liu, W. Cai, and H. Bi, "Optical absorption of copper nanoparticles dispersed within pores of monolithic mesoporous silica," *Journal of Materials Research*, vol. 17, no. 5, pp. 1125–1128, 2002.
- [26] B. M. Min, S. W. Lee, J. N. Lim et al., "Chitin and chitosan nanofibers: electrospinning of chitin and deacetylation of chitin nanofibers," *Polymer*, vol. 45, no. 21, pp. 7137–7142, 2004.
- [27] O. S. Yordem, M. Papila, and Y. Z. Menciloglu, "Effects of electrospinning parameters on polyacrylonitrile nanofiber diameter: an investigation by response surface methodology," *Materials and Design*, vol. 29, no. 1, pp. 34–44, 2008.
- [28] J. M. Deitzel, J. Kleinmeyer, D. Harries, and N. C. Beck Tan, "The effect of processing variables on the morphology of electrospun nanofibers and textiles," *Polymer*, vol. 42, no. 1, pp. 261–272, 2001.

- [29] X. Zong, K. Kim, D. Fang, S. Ran, B. S. Hsiao, and B. Chu, "Structure and process relationship of electrospun bioabsorbable nanofiber membranes," *Polymer*, vol. 43, no. 16, pp. 4403–4412, 2002.
- [30] J. Yun, K. Cho, B. Park, H.-C. Kang, B.-K. Ju, and S. Kim, "Optical heating of ink-jet printable Ag and Ag-Cu nanoparticles," *Japanese Journal of Applied Physics*, vol. 47, no. 6, pp. 5070–5075, 2008.